Dynamic Stark broadening as the Dicke narrowing effect

A. Calisti,[1,*] C. Mossé,[1] S. Ferri,[1] B. Talin,[1] F. Rosmej,[2,†] L. A. Bureyeva,[3] and V. S. Lisitsa[4]
[1]*PIIM, UMR6633, Centre Saint Jérôme, Université de Provence–CNRS, Case 232, 13397 Marseille Cedex 20, France*
[2]*UMR 7605, LULI, Université Pierre et Marie Curie, Case 128, 4 Place Jussieu, 75252 Paris Cedex 05, France*
[3]*Institute of Spectroscopy, Troitsk, Moscow Region 142190, Russia*
[4]*Russian Research Center, "Kurchatov Institute," Moscow 123182, Russia*
(Received 24 August 2009; published 26 January 2010)

A very fast method to account for charged particle dynamics effects in calculations of spectral line shape emitted by plasmas is presented. This method is based on a formulation of the frequency fluctuation model (FFM), which provides an expression of the dynamic line shape as a functional of the static distribution of frequencies. Thus, the main numerical work rests on the calculation of the quasistatic Stark profile. This method for taking into account ion dynamics allows a very fast and accurate calculation of Stark broadening of atomic hydrogen high-n series emission lines. It is not limited to hydrogen spectra. Results on helium-β and Lyman-α lines emitted by argon in microballoon implosion experiment conditions compared with experimental data and simulation results are also presented. The present approach reduces the computer time by more than 2 orders of magnitude as compared with the original FFM with an improvement of the calculation precision, and it opens broad possibilities for its application in spectral line-shape codes.

DOI: 10.1103/PhysRevE.81.016406 PACS number(s): 52.20.−j, 52.25.−b, 32.70.Jz, 32.60.+i

I. INTRODUCTION

The emitted radiation is usually one of the few observable physical quantities available to obtain information on the underlying physical processes involved in line formation in plasmas. Modeling broadening due to Stark effect of transitions from neutral or charged emitters is a complicated problem that involves a complex combination of atomic physics data, statistical mechanics, and detailed plasma physics [1]. The most difficult part of a line-broadening problem is to properly and completely identify the environment of the emitter. In particular, accounting for the fluctuations of electric fields produced at emitters, by moving electrons and ions, has been of constant interest for both the experimental and theoretical points of view since the 1960s [2]. Different methods have been developed among which the model microfield method (MMM) [3,4] and numerical simulations [5–9] and kinetic theory models such as those developed by Boerker, Iglesias, and Dufty (BID) [10] and frequency fluctuation model (FFM) [11] have proven to be the most successful. Recently, with the advances in computer technology, two-component ion plus electron plasma molecular dynamics (MD) simulations have been applied in studies devoted to spectral line shapes [12–14]. The simulations numerically solve the Schrödinger equation describing the time evolution of the emitter wave functions in the time-dependent field of electrons and ions produced by MD and then average over configurations to obtain the final result. Simulations are used as model laboratory experiments to compare with line shapes calculated by other methods or resulting from experiments. Unfortunately, this technique is time consuming and thus impractical for the modeling of today's highly complex plasma experiments. The FFM has been developed to overcome this difficulty and to permit fast calculations of the radiation emitted by complex or highly charged ions in plasmas. It relies on the hypothesis that the emitter-plasma system behaves approximately like a pseudomolecule embedded into a thermal bath. As a result, the pseudosystem can be considered to have internal states connected to each other by collisions with the bath. This simple starting point has been turned into a powerful renormalization process, called FFM, resulting, a few years ago, in a fast line-shape code called PPP [15] and a code for the computation of radiative redistribution function [16]. The validity of the FFM has been abundantly tested by comparisons with both simulations and, where available, high-precision line-shape measurements [17]. The modern state of the art in radiating plasma physics investigations deals with a complex combination of different theoretical models such as detailed atomic level population kinetics together with radiation transport phenomena in nonuniform plasmas. In this context, the FFM in its original formulation, despite its rapidity, remains too slow and, above all, too difficult to be implemented in the codes used in plasma spectroscopy. The goal of the present paper is to present a more efficient formulation of the FFM to account for dynamic effects of electric fields on atomic spectra in plasmas.

II. METHOD

The line-shape function in the radiative dipole approximation is related to the imaginary part of the Fourier-transformed dipole autocorrelation function. This can be written as a normalized Liouville space-matrix element of the response function,

$$I(\omega) = \mathrm{Im}\langle\langle d^{+}|G(\omega)|d\rho_0\rangle\rangle, \tag{1}$$

where ρ_0 is the equilibrium density-matrix operator for the active quantum system and d is the dipole operator for the

*annette.calisti@univ-provence.fr
†Also at Ecole Polytechnique, Laboratoire pour Utilisation des Lasers Intenses (LULI), Physique Atomique dans les Plasmas Denses, 91128 Palaiseau Cedex, France.

emitting quantum system. The response function, $G(z)$, is given by the one-sided Fourier transform of the bath-averaged evolution operator of the emitter $U(t,0)$,

$$G(z) = i\int_0^{+\infty} U(t,0)e^{-izt}dt = (z-L)^{-1}. \tag{2}$$

Here, L is the Liouville operator for the emitter evolution alone. If the interaction fluctuations or collisions are random, a stochastic Liouville equation (SLE) must be solved to obtain $G(z)$. In a few well-known cases, the SLE can be solved either exactly or to a good approximation. For example, an analytical solution is obtained for the impact limit in which short and rare binary collisional events occur between emitters and perturbers and the mean time between collisions is much longer than the collision time. The second example concerns the static limit where the perturbing ion microfields, acting on emitters, are constant during the radiative process and are well characterized by a probability density. In most of theoretical models of spectral line shapes in plasmas, the time dependence of the perturbation is eliminated, resulting in a spectral line shape that has pure homogeneous and inhomogeneous contributions and is described by a simple sum of independent electron-impact broadened static components. Although the electron collisions are often well described by the impact approximation, it is well known that a quasistatic treatment of the ion perturbation can lead to large errors for plasma conditions that yield substantial ion-field fluctuations. As an alternative solution, the FFM is based on the premise that a quantum system perturbed by an electric microfield behaves like a set of field dressed two-level transitions, the Stark dressed transitions (SDT). If the microfield is time varying, the transitions are subject to a collision-type mixing process (a Markov process) induced by the field fluctuations.

Suppose the system variables take the values $x_1, x_2, \cdots, x_n$ at times $t_1, t_2, \cdots, t_n$ with probability function $\phi_n(x_n,t_n;\cdots x_1,t_1)$. The changes in $x(t)$ are a Markov process when

$$\phi_n(x_n,t_n;\cdots x_1,t_1) = P(x_n t_n|x_{n-1}t_{n-1})\cdots P(x_2t_2|x_1t_1), \tag{3}$$

where $P(x_2t_2|x_1t_1)$ is the conditional probability that $x(t)$ will have the value x_2 at t_2 when $x(t_1)=x_1$. The conditional or transition-probability function satisfies the Chapman-Kolmogorov equation

$$P(x_2t_2|x_1t_1) = \sum_{x'} P(x_2t_2|x't')P(x't'|x_1t_1), \tag{4}$$

as well as

$$\sum_{x_2} P(x_2t_2|x_1t_1) = 1 \tag{5}$$

and

$$\sum_{x_1} P(x_2t_2|x_1t_1)\Phi_1(x_1,t_1) = \Phi_1(x_2,t_2), \tag{6}$$

where $\Phi_1(x,t)$ is the single-state probability distribution. At this point, it is convenient to introduce a matrix notation. If only stationary Markov processes are considered, Eq. (4) shows that it is possible to define a time-independent matrix of transition rates $\underline{\mathcal{W}}$ such as

$$\underline{P}(t) = e^{\underline{\mathcal{W}}t}. \tag{7}$$

Dividing $\underline{\mathcal{W}}$ into a diagonal matrix of inverse state lifetimes $\underline{\Gamma}$ and an off-diagonal matrix $\underline{W}$ of transition rates between different states,

$$\mathcal{W}_{x_2,x_1} = -\Gamma_{x_1}\delta_{x_2,x_1} + W_{x_2,x_1}, \tag{8}$$

the matrix elements of $\underline{P}(t)$ satisfy

$$\partial_{t_2}P(x_2t_2|x_1t_0) = -\Gamma_{x_2}P(x_2t_2|x_1t_0) + \sum_{x'} W_{x_2,x'}P(x't_2|x_1t_0). \tag{9}$$

Since $P(x_2t_2|x_1t_0)$ satisfies Eq. (5), we have

$$\Gamma_{x_1} = \sum_{x_2} W_{x_2,x_1}. \tag{10}$$

Multiplying Eq. (9) by $\Phi_1(x_1,0)$, summing over x_1, and using Eq. (6) yield a master equation which relates the single-state probability distribution to W_{x_2,x_1},

$$\partial_t\Phi_1(x_2,t) = -\Gamma_{x_2}\Phi_1(x_2,t) + \sum_{x'} W_{x_2,x'}\Phi_1(x',t). \tag{11}$$

The steady-state solution, $P_1(x)$, of this equation is then determined by

$$\Gamma_x P_1(x) = \sum_{x'} W_{x,x'}P_1(x'). \tag{12}$$

Using matrix notation, we can write the one-sided Fourier transform of $\underline{P}(t)$ as

$$\underline{P}(z) = -i(z + i\underline{W} - i\underline{\Gamma})^{-1} \tag{13}$$

so that the propagator is [18]

$$\underline{\mathcal{G}}(z) = (z + i\underline{W} - i\underline{\Gamma} - \underline{L})^{-1}. \tag{14}$$

Assuming that the rate of transitions from state x_1 to state x_2 is independent of x_1, we obtain

$$W_{x_2,x_1} = \Gamma P_1(x_2), \tag{15}$$

where Γ is a constant fluctuation rate. This transition rate matrix is referred to as the strong collision limit for velocity states in Doppler-broadening description [19] or Poisson step process in the model microfield method [3], it suggests that the cause of the change in states is so violent that in its final states, the system has no memory of its initial state. Working in the Liouville space of the dressed two-level radiators in which the basis set of eigenvectors, $\{|e,g;j\rangle\rangle\}$, is labeled by the quantum numbers of the emitters (e,g) and by the SDT label j, the line shape is written as [16]

$$I(\omega) = \mathrm{Re}\frac{1}{\pi}\sum_{kj} i\langle D_k|(\omega - \underline{L} - i\underline{\Gamma} + i\underline{W})^{-1}|D_j\rangle p_j, \tag{16}$$

where $\underline{L}$ is the Liouville operator involving the transition energies of the SDT, D_i are the matrix elements of the dipole moment for the SDT and $p_i = a_i/r^2$ (a_i being the intensity of

the SDT, i, and $r^2=\Sigma_k a_k$) is the instantaneous probability of state i; the probability of quantum radiation at the specific frequency shift due to Stark splitting of energy levels. $\underline{\Gamma}$ is the diagonal matrix of inverse state lifetimes with $\Gamma_{kj}=\Gamma\delta_{kj}=(v_{th}/d)\delta_{kj}$ (where v_{th} is the thermal velocity of perturbers and d is the mean interparticle distance) and $\underline{W}$ is the matrix of transition rates between different states such as $W_{kj}=\Gamma p_k$.

Equation (16) involves a finite matrix inversion whose size can be very large. In the original FFM [11], a renormalization process was proposed to overcome this difficulty. This process introduced an additional approximation and proved insufficient in some very complex cases. Hereafter, a formulation is presented which avoids matrix inversion, thus considerably improving the method. Defining the quasistatic propagator

$$\underline{G^s}(z)=(z-\underline{L}-i\underline{\Gamma})^{-1}, \tag{17}$$

which has only diagonal matrix elements, the total propagator $\mathcal{G}(z)$, from Eq. (14), can be written as

$$\mathcal{G}(z)=\underline{G^s}(z)-i\underline{G^s}(z)\cdot\underline{W}\cdot\mathcal{G}(z). \tag{18}$$

Introducing the previous expression in Eq. (16), we get

$$I(\omega)=\frac{r^2}{\pi}\mathrm{Re}\frac{\sum_k \frac{a_k/r^2}{i(\omega-\omega_k)+\Gamma}}{1-\Gamma\sum_k \frac{a_k/r^2}{i(\omega-\omega_k)+\Gamma}}. \tag{19}$$

All the above results are easily extended to the situation where $x(t)$ belongs to a continuum of values. In this case, the probabilities $P(x_2t_2|x_1t_1)$ and $\Phi(x,t)$, defined for discrete $x(t)$, become probability densities $p(x_2t_2|x_1t_1)$ and $\phi(x,t)$, and all sums are replaced by integrals. In this case, the probability $p_k=a_k/r^2$ is replaced by $W(\omega)d\omega$ the probability to have a radiation at a frequency in the range ω and $\omega+d\omega$ obtained in the static limit. The previous equation is then written as

$$I(\omega)=\frac{r^2}{\pi}\mathrm{Re}\frac{\int \frac{W(\omega')d\omega'}{\Gamma+i(\omega-\omega')}}{1-\Gamma\int \frac{W(\omega')d\omega'}{\Gamma+i(\omega-\omega')}}. \tag{20}$$

With $W(\omega)$ being the normalized static line shape, the main numerical work remains in the calculation of the quasistatic profile.

Note that this expression is similar to that obtained in [19] to describe the Doppler effect in the framework of a strong collision model (Dicke effect [20]),

$$I(\omega)=\frac{1}{\pi}\mathrm{Re}\frac{\int \frac{W(\vec{v})d\vec{v}}{\nu+i(\omega-\vec{k}\,.\,\vec{v})}}{1-\nu\int \frac{W(\vec{v})d\vec{v}}{\nu+i(\omega-\vec{k}\,.\,\vec{v})}}. \tag{21}$$

There, the thermal bath is composed of radiator velocity states $\vec{v}$ with the probability distribution $W(\vec{v})$. The velocity-changing collisions result in an effective jumping from one value of the atomic velocity to one other following a Markov process. The line shape is, then, transformed from nonuniform Gaussian to uniform Lorentzian line shape with the effective line width equal to

$$\gamma_D\propto\frac{\Delta\omega_D^2}{\nu} \tag{22}$$

where $\Delta\omega_D$ is the Doppler width of the line and ν is the velocity-changing collision frequency. We will come back on this analogy in the following section.

As it has been noticed previously, electrons in plasmas are well described by the impact approximation. The quantum-emitter system evolution operator in Eq. (2), then, contains in the Liouville operator a non-Hermitian homogeneous electron-impact broadening contribution, resulting in static Stark components (SDT) characterized by a complex frequency $\omega_k-i\gamma_k$ and intensity a_k+ic_k. The line-shape function for a given transition with n SDT is, then, written as

$$I(\omega)=\frac{r^2}{\pi}\mathrm{Re}\frac{\sum_k \frac{(a_k+ic_k)/r^2}{i(\omega-\omega_k)+\gamma_k+\Gamma}}{1-\Gamma\sum_k \frac{a_k/r^2}{i(\omega-\omega_k)+\gamma_k+\Gamma}}. \tag{23}$$

If the condition $c_k\ll a_k$ is fulfilled and γ_k is weakly k dependent, $\gamma_k=\gamma$. Then, Eq. (23) can be written as

$$I(\omega)=\frac{r^2}{\pi}\mathrm{Re}\frac{\int \frac{W(\omega')d\omega'}{\Gamma+\gamma+i(\omega-\omega')}}{1-\Gamma\int \frac{W(\omega')d\omega'}{\Gamma+\gamma+i(\omega-\omega')}}. \tag{24}$$

As γ does not depend on the frequency of the emitting atom, Eq. (24) can be represented as the convolution of a lorentzian function and function (20) which defines the line contour when $\gamma=0$,

$$I(\omega)=\int d\omega''\frac{\gamma/\pi}{\gamma^2+(\omega-\omega'')^2}\mathrm{Re}\left\{\frac{r^2}{\pi}\frac{\int \frac{W(\omega')d\omega'}{\Gamma+i(\omega''-\omega')}}{1-\Gamma\int \frac{W(\omega')d\omega'}{\Gamma+i(\omega''-\omega')}}\right\}. \tag{25}$$

III. RESULTS AND DISCUSSION

The hydrogenic argon Lyman-α transition, including fine structure, in a weakly coupled proton plasma, is considered first in this section to illustrate the effects of ion dynamics on spectral line shapes and the analogy with Dicke narrowing effect. The quantum system involves the four levels $1S_{1/2}$, $2S_{1/2}$, $2P_{1/2}$, and $2P_{3/2}$. This case is very advantageous because the spectrum involves two patterns resulting from both linear and quadratic Stark splitting associated, respectively, with the two fine-structure components $1S_{1/2}$-$2P_{1/2}$ and $1S_{1/2}$-$2P_{3/2}$.

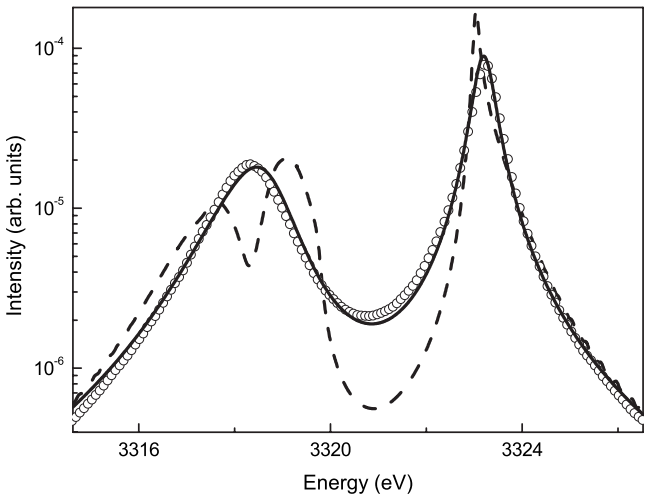

FIG. 1. Lyman-α line with fine structure at $N_e=1.5\times10^{23}$ cm^{-3} and $T_e=10^7$ K. Comparisons between static profile (dash line), dynamic profile (full line) and molecular dynamics simulation calculation (circles).

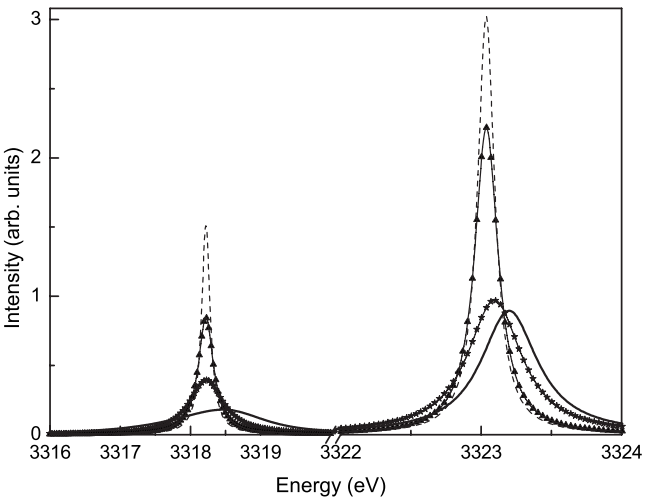

FIG. 2. Lyman-α line with fine structure at $N_e=1.5\times10^{23}$ cm^{-3} and $T_e=10^7$ K. Dynamic profile with different fluctuation rates, Γ (full line: same as Fig. 1 with $\Gamma=1.5$, stars: $\Gamma=10$, and triangles: $\Gamma=100$) compared to unperturbed profile obtained with a zero ionic electric field (dash line).

Figure 1 shows the Lyman-α profile for hydrogenlike argon in protons without Doppler broadening calculated for the plasma conditions $N_e=1.5\times10^{23}$ cm^{-3} and $T_e=10^7$ K. Three different results have been plotted in logarithm scale: the static profile (dash line), the dynamic profile obtained with the new formulation of the FFM (full line) and the simulation result (circles). In these simulations, a representative set of ionic electric-field histories is generated by using molecular dynamics technique, then, the time-depending histories are used in a step-by-step integration of the Schrödinger equation and the final result is obtained averaging over the set of histories. Results from simulations are considered as benchmark, as they rely neither on impact nor static approximation. Comparisons with numerical simulations show a very good agreement. The two fine-structure components show different behaviors. Due to linear Stark effect on the $1S_{1/2}$-$2P_{1/2}$, two resonances appear in the static approximation which are mixed and merged into a single one by ion dynamics. On the $1S_{1/2}$-$2P_{3/2}$ the main feature due to quadratic static Stark effect seems to be enhanced by ion dynamics and the dynamic profile appears broaden and shifted. In all the cases, it can be noticed that, as expected, the wings are well represented by the static profile. The FFM method describes continuously the region between the static limit which corresponds to a zero fluctuation rate and the fast fluctuation limit. In the limit of an infinitely rapid ion micro field fluctuation, the effect of the perturbation disappears and the line components collapse to the center of gravity. This is illustrated in Fig. 2 where the Lyman-α profile is plotted for different values of the fluctuation rate and compared with the unperturbed line corresponding to a zero ionic electric field. As we can see, even though in a first stage the profile is broadened, an increase in the fluctuation rate results in a narrowing of the profile. This effect is the same as Dicke narrowing where the rapid collisionnal mixing of velocity components causes a collapse of the Doppler line shape.

The second example concerns Stark broadening of atomic hydrogen high-n series emission lines which have been used for spectroscopic measurements of plasma density in laboratory experiments [21]. In Ref. [21], a multichannel spectroscopic diagnostic and the corresponding analysis for divertor electron-density measurements using Stark-broadened Balmer and Paschen emission lines originating from $n=7-13$ levels have been developed. It has been shown that the Paschen line profiles are an attractive recombining divertor density diagnostic for a burning plasma experiment. Diagnostics are based on comparisons between experimental data and theoretical results that must be as accurate as possible.

Figure 3 shows the static and dynamic profiles for the Balmer 10–2 and the Paschen 10–3 transitions for an electronic density $N_e=10^{14}$ cm^{-3} and a temperature $T_e=10$ eV corresponding to observations performed in the National Spherical Torus Experiment detached divertor region. These

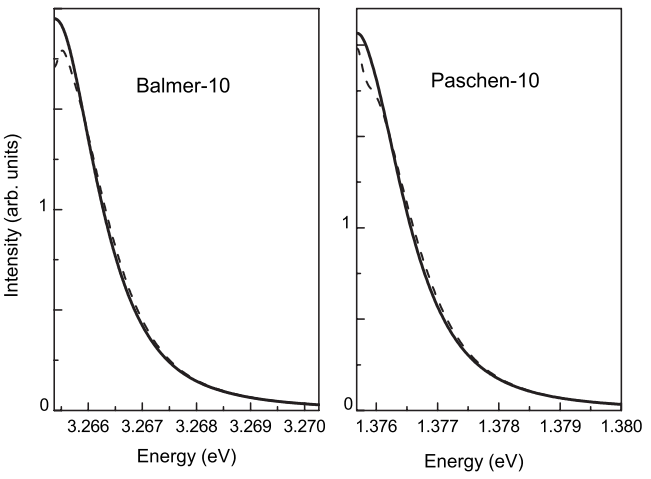

FIG. 3. Balmer 10–2 and Paschen 10–3 lines at $N_e=10^{14}$ cm^{-3} and $T_e=10$ eV. Comparisons between static profile (dash line) and dynamic profile (full line).

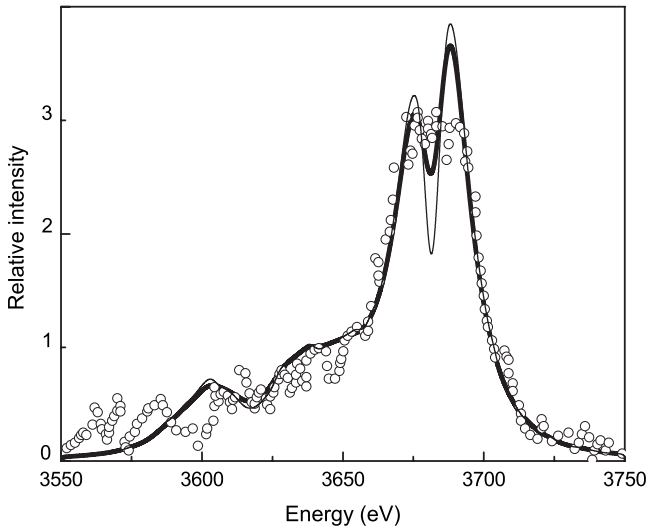

FIG. 4. Ar XVII $1s^2$-$1s3p$ ^1P at $N_e=1.2\times10^{24}$ cm^{-3} and $T_e=700$ eV. Comparison of the full ion dynamics calculation including the Li-like satellites (bold full line) with the experimental data (circles) and the static profile (thin full line).

calculations, which were impracticable or very difficult to perform without approximation, have been done in a few seconds. In addition, as no matrix inversion is required, the results are more accurate.

The method presented here is not limited to hydrogen spectra. It is particularly useful when a Stark-broadened impurity profile is used for plasma diagnostic purposes. This line-shape computation in hot dense plasma conditions can be difficult and very time consuming. This is because the spectra of interest are not limited to the simplest hydrogenlike or heliumlike ionic lines but include also lines radiated by complex three or more electron ions (dielectronic satellites for example).

The third example concerns the Helium-β line of argon, Ar XVII $1s^2$-$1s3p$ ^1P, and the associated lithiumlike dielectronic satellite lines, in deuterium for plasma conditions typical of inertial confinement fusion experiments [22]. In these experiments, rare-gas atoms are introduced in trace amounts as a nonperturbing dopant in the gas fill of the microspheres of the implosion experiments. The profiles of the lines emitted by the rare-gas ions are then used as a diagnostic by comparing the experimental results with theoretical predictions. Figure 4 displays a comparison of the full ion dynamics calculation of the helium-β line including the Li-like $2l3l'$ and $3l3l'$ dielectronic satellite lines for Argon impurities in deuterium at $N_e=1.2\times10^{24}$ cm^{-3} and $T_e=700$ eV with the experimental data [22] and the static profile. It has been shown in Ref. [22] that ion dynamics effects cannot be considered as the unique cause of the filling of the line central feature. Even though, ion dynamics effects improve the comparison with experimental data, some discrepancies remain and their study is not the subject of this paper (for more details see Ref. [22]). Calculations of ion dynamics effects on Li-like satellite lines involve hundred thousands of Stark components, and the calculation with the original FFM was extremely difficult or impracticable. The present FFM formulation permits to get the ion profile in a couple of minutes on a workstation.

IV. CONCLUSION

A very fast method to account for charged particle dynamics effects in calculations of spectral line shapes has been presented and tested by comparisons with numerical simulations. Comparisons with experimental data illustrate the need to calculate ion dynamics effects for line shapes emitted by complex atomic systems.

The method is based on a formulation of the FFM, which provides an expression of the dynamic line profile as a functional of the static frequency distribution and a unique parameter, the fluctuation rate. This expression is similar to that obtained to describe the Doppler effect in the framework of strong collision models (Dicke effect). In this model, a Markovian mixing process of velocities mimics the velocity-changing collision effect, on the Doppler profile, which result in the line-shape transformation from nonuniform Gaussian to uniform Lorentzian line shape when the collision rate increases. The same description of transition from inhomogeneous (static) to homogeneous (Lorentzian or fast fluctuation limit) can be done for Stark profiles. The main numerical work is the calculation of the static profile. It can be obtained by different analytical or numerical methods. Different models [23,24] have been proposed in order to facilitate the calculations of line shapes of highly excited (Rydberg) hydrogen atoms and ions important for many topics in plasma physics and astrophysics. Some very sophisticated code have been developed, PPP-TOTAL code [15] or MERL multielectron-radiator line shape code [25], for example, to calculate spectral line shape emitted by complex multielectronic emitters.

This work opens possibilities for ultra fast calculations of dynamic line shapes for arbitrary values of plasma parameters (densities and temperatures). It is of special importance for strongly nonuniform plasmas where one needs to calculate spectra for a wide domain of plasma parameters. It is the case both for laser driven plasmas and magnetically confined (especially divertor) plasma conditions. Another application concerns Stark-Zeeman profiles for which, ion dynamics calculations are, strongly, facilitated by using this new formulation. These profiles are of great interest for astrophysics and thermonuclear fusion physics.

ACKNOWLEDGMENTS

Authors thank the anonymous referee for his/her very helpful comments and suggestions. The work is partially supported by RFBR Grant No. 08-02-00294-a and Federal Target Program "Academic and Teaching Staff of innovation Russia 2009–2012."

[1] H. Griem, *Spectral Line Broadening by Plasma* (Academic Press, New York, 1974).
[2] H. Griem, *Principles of Plasma Spectroscopy* (Cambridge University Press, Cambridge, 1997).
[3] A. Brissaud and U. Frisch, J. Quant. Spectrosc. Radiat. Transf. **11**, 1767 (1971).
[4] A. Brissaud and H. Frisch, J. Math. Phys. **15**, 524 (1974).
[5] R. Stamm, E. W. Smith, and B. Talin, Phys. Rev. A **30**, 2039 (1984).
[6] R. Stamm, B. Talin, E. L. Pollock, and C. A. Iglesias, Phys. Rev. A **34**, 4144 (1986).
[7] J. Seidel, *Spectral Line Shapes* (Deepack, Hampton, VA, 1987), Vol. 4, p. 57.
[8] G. C. Hegerfeldt and V. Kesting, Phys. Rev. A **37**, 1488 (1988).
[9] V. Cardeñoso and M. A. Gigosos, Phys. Rev. A **39**, 5258 (1989).
[10] D. B. Boercker, C. A. Iglesias, and J. W. Dufty, Phys. Rev. A **36**, 2254 (1987).
[11] B. Talin, A. Calisti, L. Godbert, R. Stamm, R. W. Lee, and L. Klein, Phys. Rev. A **51**, 1918 (1995).
[12] B. Talin, E. Dufour, A. Calisti, M. A. Gigosos, M. A. Gonzalez, T. del Rio Gaztelurrutia, and J. W. Dufty, J. Phys. A **36**, 6049 (2003).
[13] E. Dufour, A. Calisti, B. Talin, M. A. Gigosos, M. A. Gonzalez, and J. W. Dufty, J. Quant. Spectrosc. Radiat. Transf. **81**, 125 (2003).
[14] E. Stambulchik, D. V. Fisher, Y. Maron, H. R. Griem, and S. Alexiou, High Energy Density Phys. **3**, 272 (2007).
[15] A. Calisti, L. Godbert, R. Stamm, and B. Talin, J. Quant. Spectrosc. Radiat. Transf. **51**, 59 (1994).
[16] C. Mossé, A. Calisti, R. Stamm, B. Talin, R. W. Lee, and L. Klein, Phys. Rev. A **60**, 1005 (1999).
[17] L. Godbert-Mouret, T. Meftah, A. Calisti, R. Stamm, B. Talin, M. Gigosos, V. Cardeñoso, S. Alexiou, R. W. Lee, and L. Klein, Phys. Rev. Lett. **81**, 5568 (1998).
[18] B. Talin and L. Klein, Phys. Rev. A **26**, 2717 (1982).
[19] S. G. Rautian and I. I. Sobelman, Sov. Phys. Usp. **9**, 701 (1967).
[20] R. H. Dicke, Phys. Rev. **89**, 472 (1953).
[21] V. A. Soukhanovskii, D. W. Johnson, R. Kaita, and L. Roquemore, Rev. Sci. Instrum. **77**, 10F127 (2006).
[22] N. C. Woolsey, A. Asfaw, B. Hammel, C. Keane, C. A. Back, A. Calisti, C. Mossé, R. Stamm, B. Talin, J. S. Wark, R. W. Lee, and L. Klein, Phys. Rev. E **53**, 6396 (1996).
[23] C. Mossé, A. Calisti, S. Ferri, B. Talin, L. A. Bureyeva, and V. S. Lisitsa, *Spectral Line Shapes: The 19th International Conference on Spectral Line Shapes*, AIP Conf. Proc. No. 1058(AIP, New York, 2008), p. 63.
[24] E. Stambulchik and Y. Maron, J. Phys. B **41**, 095703 (2008).
[25] R. C. Mancini, D. P. Kilcrease, L. A. Woltz, and C. F. Hooper, Jr., Comput. Phys. Commun. **63**, 314 (1991).